Probabilistic Temporal Subspace Clustering

Behnam Gholami
Department of Computer Science
Rutgers University
bb510@cs.rutgers.edu

Vladimir Pavlovic
Department of Computer Science
Rutgers University
vladimir@cs.rutgers.edu

Abstract

Subspace clustering is a common modeling paradigm used to identify constituent modes of variation in data with locally linear structure. These structures are common to many problems in computer vision, including modeling time series of complex human motion. However classical subspace clustering algorithms learn the relationships within a set of data without considering the temporal dependency and then use a separate clustering step (e.g., spectral clustering) for final segmentation. Moreover, these, frequently optimization-based, algorithms assume that all observations have complete features. In contrast in real-world applications, some features are often missing, which results in incomplete data and substantial performance degeneration of these approaches. In this paper, we propose a unified non-parametric generative framework for temporal subspace clustering to segment data drawn from a sequentially ordered union of subspaces that deals with the missing features in a principled way. The non-parametric nature of our generative model makes it possible to infer the number of subspaces and their dimension automatically from data. Experimental results on human action datasets demonstrate that the proposed model consistently outperforms other state-of-the-art subspace clustering approaches.

1. Introduction

High dimensional data are ubiquitous in many machine learning applications. Modeling such data using low dimensional representations can potentially reduce the computation time and memory requirements of the algorithms used to extract information from the data. A standard assumption in many applications is that high dimensional data lie on the union of a small number of much lower dimensional subspaces. The goal of subspace clustering is to simultaneously cluster data points into multiple subspaces and find the corresponding subspace for each cluster.

Mathematically, subspace clustering (SC) [7, 27, 45, 60] is defined as follows: Let $\boldsymbol{X} \in \mathbb{R}^{d \times N}$ be the data matrix consisting of N data points $\{x_n \in \mathbb{R}^d\}_{n=1}^N$ assumed be drawn from a union of S linear subspaces Φ_s of unknown dimension $K_s = dim(\Phi_s)$, with $0 < K_s < d$. The subspace clustering attempts to infer the number of subspaces S, the subspaces $\{\Phi_s\}_{s=1}^S$, their dimensions $\{K_s\}_{s=1}^S$, and the clustering of the data points x_n into these subspaces.

Subspace clustering has achieved outstanding performance in many machine learning applications, such as face clustering [61], motion segmentation [8, 23], document clustering [34], etc, and many SC algorithms have been developed, including Sparse and Low Rank Methods [7, 24, 29, 54], algebraic methods [42], and statistical methods [2, 13, 21, 49].

Recent work on low rank representation (LRR) [24–26, 30], sparse representation (SSC) [6, 7], least square regression (LSR) [29], and their extensions [1, 3–5, 9, 11, 12, 14–16, 18, 20, 22, 28, 31–33, 35, 37, 38, 47, 48, 50, 53, 55–59, 59, 62] have attracted much attention in subspace clustering. Low-rank/sparse methods attempt to find a new representation $\boldsymbol{Z} \in \mathbb{R}^{K \times N}$ of the data and then apply a spectral clustering method on the learned representation $\boldsymbol{Z}$. Sparse subspace clustering (SSC) algorithms [6, 7] enforce a sparsity constraint on the representation $\boldsymbol{Z}$ to recover the multi-subspace structure. Low-rank representation (LRR) algorithms [24, 26] impose low rank constraint on $\boldsymbol{Z}$ and least-square regression (LSR) [29] uses l_2 norm regularizer for $\boldsymbol{Z}$.

Statistical methods [2, 13, 21, 49] usually model the data points using a mixture of probabilistic PCAs. Due to the probabilistic nature of the statistical methods, they are more robust to noise and outliers, in contrast to the low-rank/sparse methods.

One of the shortcomings of all of the above methods is that they generally assume all data points are drawn independently from multiple subspaces. Hence, they fail to exploit the information explicitly encoded into the time series. For example, in a video sequence, where the goal is to cluster the frames that belong to the same scene, it is reasonable to assume that the consecutive frames belong to one and the same scene, until a scene change occurs forming temporally consistent clusters.

Very recently, some subspace clustering methods have been proposed [23, 40, 52] that can take advantage of order information embedded in the data points to improve the clustering performance. Wu et al. [52] proposed a SC algorithm for sequential data by imposing a quadratic normalizer on the sparse coefficients to model the temporal correlation among the data points. Additionally, a block-diagonal prior for the spectral clustering affinity matrix is incorporated into the model to improve the clustering accuracy. Tierney et al. [40] proposed an Ordered Subspace Clustering (OSC) method by introducing a $l_{1,2}$ norm as a regularizer for the sparse representations that not only maintains the sparsity of the learned representation, but also forces the consecutive frames to have similar representation. Motivated by the well-known Laplacian regularization technique, Li et al. [23] proposed a temporal subspace clustering (TSC) method that uses a temporal Laplacian regularization function to encode the sequential relationships in time-dependent data. They also learn a non-negative dictionary from the data rather than using the data itself as the dictionary to obtain more expressive coding.

There are two major problems with the above temporal subspace clustering methods. First, these methods are not designed to deal with missing features in a principled way. More precisely, when some entries of the data points are corrupted or missing (e.g., commonly some marker sets of multiple body parts are missing during motion capture in motion segmentation applications), these methods cannot explicitly and efficiently deal with the corrupted data. Second, the performance of these optimization-based (non-probabilistic) methods depends on a set of free parameters that need to be carefully tuned using cross-validation or other parameter tuning techniques, which increases both the computational complexity and the sensitivity of these methods.

To address the above-mentioned problems, we propose a unified probabilistic framework for temporal subspace clustering where temporal dependencies are modeled using Gaussian Process (GP) [51] priors (whose covariance function controls the desired dependence) on to the data point's clustering indices that can effectively deal with missing data. By employing Griffiths-Engen-McCloskey (GEM) distribution [17] defined via the stick breaking construction as the prior distribution on the clustering indices, our model is capable of inferring the number of the subspaces (clusters) automatically from the data. Moreover, by incorporating the Bernoulli process [39] into our model, we are able to concurrently learn the dimensionality of the subspaces from the data. Given a set of ordered data points, we also develop an EM algorithm to learn the complete set of parameters from the data itself.

The rest of this paper is organized as follows. We present the proposed temporal subspace clustering framework in Section 2. In Section 3, we develop an EM algorithm to learn the parameters of the proposed model. Experimental results are presented in Section 4. Finally, we conclude our work in Section 5.

2. Proposed Method

2.1. Problem Formulation

Let $\boldsymbol{X} = [x_1, x_2, ..., x_N]_{d\times N}$ be a sequence of d-dimensional time-series data, where the n-th data point $x_n (n = 1, ..., N)$ is sampled at time t_n. We assume that the data points are generated via a mixture of S subspaces. Mathematically, each data point x_n can be represented as $\mathcal{M} = (c_n, \{\boldsymbol{\Phi}_s, \mu_s, w_{s,n}, \alpha_s\}_{s=1}^S)$, where $\boldsymbol{\Phi}_s \in \mathbb{R}^{d\times K_s}$ and $\mu_s \in \mathbb{R}^d$ specify the set of bases and the center of the s-subspace respectively, $w_{s,n}$ is the latent representation (projection) of x_n in subspace s, α_s indicates the noise precision parameter and $c_n \in \{1, 2, ..., S\}$ is the cluster index for the data point x_n. By defining $\boldsymbol{\Phi} = \{\boldsymbol{\Phi}_s\}$ and $\boldsymbol{\mu} = \{\mu_s\}$, the likelihood of x_n given $\mathcal{M}$ becomes

$$p(x_n|\mathcal{M}) = \sum_{s=1}^{S} p(c_n = s)p(x_n|c_n = s, w_{s,n}, \boldsymbol{\Phi}, \boldsymbol{\mu}, \alpha_s),$$

where $p(c_n = s)$ encodes a mixture probability distribution over the S clusters (subspaces), and $p(x_n|c_n = s, w_{s,n}, \boldsymbol{\Phi}, \boldsymbol{\mu})$ is defined as

$$p(x_n|c_n = s, w_{s,n}, \boldsymbol{\Phi}, \boldsymbol{\mu}) = \mathcal{N}(x_n; \boldsymbol{\Phi}_s w_{s,n} + \mu_s, \alpha_s^{-1}\boldsymbol{I}), \tag{1}$$

where $\boldsymbol{I}$ denotes the *identity* matrix of size d.

In the proposed model, we assume the number of subspaces S and their dimensionality $\{K_s\}_{s=1}^S$ are unknown apriori. To address the problem of inferring S and $\{K_s\}_{s=1}^S$, we employ the GEM distribution [17] and the Bernoulli process [39], respectively.

GEM distribution with parameter η, GEM(η), can be defined as a distribution over a countably infinite number of objects (for simplicity, natural numbers $\mathbb{N} = \{1, 2, ...\}$) as

$$p(c = s) = \beta_s, \beta_s = v_s \prod_{l=1}^{s-1}(1-v_l), v_s \sim Beta(1, \eta), s \in \mathbb{N}$$

where β_s is the mixing proportion defined by recursively breaking a unit-length stick into an infinite number of pieces. We use GEM(η) as a prior distribution over the cluster indices, $p(c_n = s) = \beta_s$, as it apriori endows the model with a countably infinite number of subspaces. Since β_s's decrease exponentially quickly, only a small number of subspaces will be used to fit the finite available data, with the appropriate number of subspaces automatically revealed by the data itself.

In order to infer the dimensionality K_s of each subspace from the observed data, we introduce an auxiliary, latent

binary vector $z_s \in \{0,1\}^{K_s}$ for each subspace $\mathbf{\Phi}_s$, where the non-zero entries of z_s specify the bases of that subspace i.e., $K_s = \sum_k z_{s,k} = dim(\Phi_s)$. Consequently, the model in Eq. 1 is reformulated as

$$p(x_n|c_n = s, z_s, w_{s,n}, \mathbf{\Phi}, \boldsymbol{\mu}, \alpha_s) = \mathcal{N}\big(x_n; \mathbf{\Phi}_s(z_s \odot w_{s,n}) + \mu_s, \alpha_s^{-1}\boldsymbol{I}\big)$$

where $\odot$ denotes the element-wise multiplication operator. Consequently, all data points $\{x_n\}$ drawn from a given cluster (subspace) s share the same set of important bases of the subspace $\mathbf{\Phi}_s$ defined by z_s, but each draw from a given cluster has unique weights $w_{s,n}$.

Using a probabilistic hierarchical framework, we place a non-parametric prior distribution on each binary vector z_s by introducing auxiliary variables $\{\mathbf{\Pi}_s = \{\pi_{ks}\}_{k=1}^{K}\}_{s=1}^{\infty}$ drawn from the Beta distribution as

$$\pi_{ks} \sim Beta(a/K, b(K-1)/K)$$

where a, b are the hyper-parameters and the integer K the largest possible dimension for z_s (by letting $K \to \infty$, the length of the binary code z_s can be learned from the observed data points [39], hence, we can learn the number of the bases for each subspace using data itself). Then, we model the binary vector z_s as a random sample from the Bernoulli process parameterized by $\mathbf{\Pi}_s$

$$z_s \sim \prod_{k=1}^{K} Ber(z_{ks}; \pi_{ks}), \quad k = 1, ..., K, \ s = 1, 2, ...,$$

where z_{ks} denotes the k-th element of the binary vector z_s and Ber denotes the Bernoulli distribution. To complete our probabilistic generative model, we model the weights $\{w_{s,n}\}$, by a zero-mean Gaussian distribution with precision value $\gamma_{s,n}$.

2.2. Temporally consistent clustering prior

An important problem with considering the GEM distribution as the prior distribution over the clustering indices $\{c_n\}$ is that the Beta-distributed random weights (stick weights) $\{\beta_s\}$ are shared among all data points, which is generally inappropriate for the time-dependent data. For example, one may wish to explicitly impose the belief that the nearby data points in the time domain are more likely to belong to the same subspace. We incorporate such prior belief into (2.1) by means of a GP on a 1-D temporal space by proposing the following temporal dependent stick weights for the GEM distribution. We call our prior model the Gaussian Process GEM (GP-GEM).

$$p(c_n = s) = \beta_s^n, \ \ \beta_s^n = \sigma(f^s(t_n)) \prod_{l=1}^{s-1} (1 - \sigma(f^l(t_n))), \quad n = 1, ..., N, \ s = 1, 2, ... \qquad (2)$$

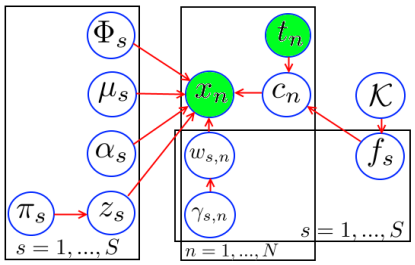

Figure 1. The graphical representation of the proposed temporal subspace clustering model (shaded circles indicate observations).

where $f^s(t) \sim GP(m(t), \mathcal{K}(t, t'))$, $f^s(t_n)$ is the value of the function $f^s(.)$ evaluated at time frame t_n of the n-th data point, and $\sigma(.)$ denotes the sigmoid function $(\sigma(x) = 1/(1 + \exp(-x)))$. The functions $\{f^s(.)\}_{s=1}^{\infty}$ are drawn from a GP with the mean function $m(.)$, which we take equal to 0 for simplicity, and the covariance function $\mathcal{K}(.,.)$. It is easy to show that the proposed prior distribution on each cluster index c_n is still a valid GEM distribution. By selecting an appropriate form of the kernel function $\mathcal{K}(t_i, t_j)$, which diminishes by increasing the distance between t_i and t_j, the proposed GEM distribution in Eq. 2 allows for obtaining prior probabilities for the clusters that depend on the values of the temporal locations $\{t_n\}_{n=1}^{N}$. Indeed, the closer the locations t_i and t_j are, the more correlated the corresponding $f^s(t_i)$ and $f^s(t_j)$ values should be, hence, the more similar the corresponding stick weights β_s^i and β_s^n are. Thus, the GP-GEM prior promotes, by construction, clustering of temporally adjacent data points.

The graphical representation of the proposed model is shown in Fig. 1. For computational simplicity, we truncate the GEM distribution in Eq. 2 to S term with $\beta_S^n = 1 - \sum_{s=1}^{S-1} \beta_s^n$, with properties of this truncation discussed in [17].

2.3. Choice of Kernel

Since the proposed GP-GEM model is constructed using Gaussian processes there is great flexibility in the choice of covariance function (kernel). For instance, one could simply use the **squared exponential** (SE) function of the form $\mathcal{K}(t_i, t_j) = \exp\{-\eta(t_i - t_j)^2\}$, where η denotes the length scale parameter [51]. Unfortunately, using unstructured arbitrary covariance functions is costly, scaling as $O(N^3)$ time because of the $N \times N$ matrix inversion (see Section 3). Since $\{t_n\} \in \mathbb{R}$ and $t_1 < t_2 < \cdots < t_N$, we propose the covariance function $\mathcal{K}(t_i, t_j) = \exp\{-\eta|t_i - t_j|\}$, whose inverse evaluated at the data points $\{t_n\}_{n=1}^{N}$[1] is a *tridiagonal* matrix, hence, $\mathbb{K}^{-1}$ can be computed in $O(N)$ time [36]. Intuitively, this **Ornstein-Uhlenbeck** kernel induces the so-called *Markovian dependence* property on f. More precisely,

[1] we use the notation $\mathbb{K}$ to denote the $N \times N$ Gram matrix of the Gaussian process f obtained by evaluating $\mathcal{K}(\cdot, \cdot)$ at $\{t_n\}_{n=1}^{N}$.

the value of the function $f(t_i)$ at t_i will not depend on any other point except for its *immediate neighbors* (according to t_i) $f(t_{i-1})$ and $f(t_{i+1})$, a reasonable assumption for a time-dependent data.

3. Non-parametric EM Estimation Algorithm

In this section, we develope a novel non-parametric EM algorithm for our proposed model. The approach resembles the standard EM algorithm yet still possesses the nonparametric nature in order to address the complexity of the model selection (infer both the number of subspaces and their dimensionality directly from the data). For this purpose, we consider $\{w_{s,n}\}$, and $\{\pi_s\}$ as latent (hidden) variables. By denoting $\mathcal{T} = \{t_n\}_{n=1}^N$, the goal of the EM algorithm is to maximize the following joint likelihood

$$p\big(\boldsymbol{X}, \mathcal{T}, \{\boldsymbol{\Phi}_s, \mu_s, z_s, \alpha_s, \gamma_{s,n}, c_n, f^s\}_{s=1,n=1,}^{S,N}, \eta\big),$$

by integrating out $\{w_{s,n}, \pi_s\}$. By denoting Θ as the set of parameters and Ω as the set of latent variables, this can be accomplished by maximizing the following lower bound on the log likelihood:

$$\log p(\boldsymbol{X}, \mathcal{T}, \Theta) \geq \log \mathbb{E}_{q(\Omega)}[\log p(\boldsymbol{X}, \mathcal{T}, \Theta, \Omega)] - \mathbb{E}_{q(\Omega)}[\log q(\Omega)],$$

where $q(\Omega)$ is the approximate posterior distribution over the set of latent variables Ω and $\mathbb{E}_q[.]$ denotes the expectation over the distribution q. For our framework to yield a computationally effective inference method, we use a factorized variational distribution

$$q(\Omega) = \prod_{s=1}^{S} \prod_{n=1}^{N} q(w_{s,n}) \prod_{k=1}^{K} q(\pi_{ks}),$$

where we iteratively update the posterior distribution $q(\Omega)$ in the **E** step and update the parameters Θ in the **M** step using the coordinate ascent algorithm. For simplicity, we also fix a single K for all the subspaces. If S and K are large enough (see Section 4), the analyzed data will reveal less than S subspaces and K bases for each subspace, respectively.

The difficulty of applying the EM algorithm for this model lies with the logistic function in (2) which makes the update equations for $\{f^s\}_{s=1}^S$ to have non-analytic form. To address this issue, one can place an exponential lower bound on the logistic functions based on the convex duality theorem [19]. Using this theorem, a variational lower bound for the logistic sigmoid function is obtained in the form of [19]

$$\frac{1}{1+exp(-x)} \geq \sigma(\xi) exp\Big((x-\xi)/2 - \lambda(\xi)(x^2-\xi^2)\Big),$$

where

$$\lambda(\xi) = \frac{-1}{2\xi}\Big(\frac{1}{1+exp(-\xi)} - \frac{1}{2}\Big).$$

and ξ is the variational parameter that should be optimized to get the tightest bound. In the proposed EM algorithm, we optimize the factorized variational distribution $q(\Omega)$ in the E-step and maximizes the parameters Θ in the M-step. Detailed update equations of the proposed non-parametric EM algorithm made available in the Supplementary Material.

3.1. Missing Data

One of the main advantages of our probabilistic formulation of temporal subspace clustering is the flexibility of allowing missing data. Generalization of the proposed EM algorithm to handle missing data is straightforward and follows [10]. The only modifications come in the form of adjusted terms for data summaries. For example, in updating the precision parameters $\{\alpha_s\}$, the term $\big\|x_n - \mu_s - \boldsymbol{\Phi}_s(z_s \odot w_{s,n})\big\|^2$ becomes

$$\sum_{\zeta \in F} \big(x_{n,\zeta} - \mu_{s,\zeta} - \boldsymbol{\Phi}_{s,\zeta}(z_s \odot w_{s,n})\big) \times \big(x_{n,\zeta} - \mu_{s,\zeta} - \boldsymbol{\Phi}_{s,\zeta}(z_s \odot w_{s,n})\big),$$

where $\odot$ denotes the element-wise multiplication operator, F is the index set of the observed (non-missing) features for the data point x_n, $x_{s,\zeta}$ is the value of the present feature, $\mu_{s,\zeta}$ is the ζ-th element of the vector μ_s and $\boldsymbol{\Phi}_{s,\zeta}$ is the ζ-th row of the matrix $\boldsymbol{\Phi}_s$. Similar expressions can be derived for other data-dependent parameters.

For reconstruction purposes, given an input x_i having missing features, our model computes the reconstruction of x_i as

$$\hat{x}_i = \mathbb{E}_{p(x_i|\Theta)}[x_i]$$

where

$$p(x_i|\Theta) = \int \mathcal{N}\big(x_i; \boldsymbol{\Phi}_s(z_s \odot w_{s,i}) + \mu_s, \alpha_s^{-1}\boldsymbol{I}\big) \times q(w_{s,i})\, dw_{s,i}$$

where s is the inferred cluster index for x_i ($c_i = s$), and $q(w_{c_i,i})$ is the variational posterior distribution of $w_{s,i}$. Since $p(x_i|\Theta)$ cannot be computed in closed form, we approximate $q(w_{s,i})$ with its mean $\mathbb{E}_{q(w_{s,i})}[w_{s,i}]$ in the above equation. Hence, $\hat{x}_i$ is computed in closed-form as

$$\hat{x}_i = \Phi_s(z_s \odot \mathbb{E}[w_{s,i}]) + \mu_s$$

4. Experimental Results

In this section, we compare our approach with several state-of-the-art subspace clustering approaches on three public human action and gesture datasets, including the Carnegie Mellon Motion Capture (Mocap) dataset, available at http://mocap.cs.cmu.edu), Ballet Action (Ballet) dataset http://www.humansensing.cs.cmu.edu/mad, and UMD Keck body-gesture (Keck) dataset

Table 1. Statistics of various Subjects of Mocap dataset (S-x denotes the Subject x).

	S-13	S-49	S-54	S-80	S-113
# activity	5	3	7	8	12
# instance	1701	811	1616	1877	2842
# feature	62	62	62	62	62

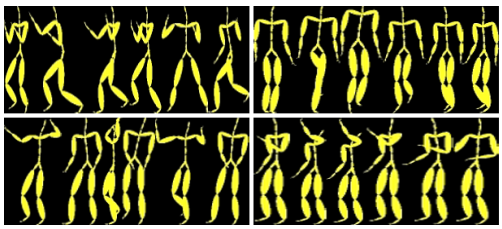

Figure 2. Four activities performed by subject 13 in the Mocap dataset: *Boxing*, *Climb three steps*, *Laugh*, and *Drink soda*.

Figure 3. Sample frames from the Ballet data set. From left to right and top to bottom: Left-to-right hand opening, right-to-left hand opening, standing hand opening, leg swinging, jumping, turning, hopping, and standing still.

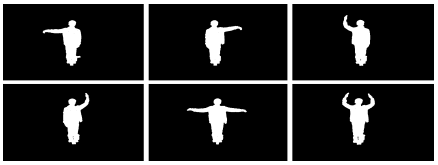

Figure 4. Sample gestures from the Keck dataset.

http://www.umiacs.umd.edu/zhuolin/Keckgesturedataset.html and one video scene segmentation datasets[2].

Mocap dataset contains 149 subjects performing several activities, from which we randomly selected 5 subjects consisting of different trials, where each trial comprises multiple activities (we selected 5 to 12 activities for each subject). Fig. 2 shows a few snapshots of some of the activities (*Boxing, Drink soda, Laugh, Climb three steps*) for subject 13. The statistics of various subjects used in the experiments are summarized in Table 1.

For the Mocap datasets, we are given sensor measurements at multiple joints of the human body (62 positions and joint angles) captured at different time instances. The goal is to segment the sensory data so that each cluster corresponds to the same activity. Here, each data point corresponds to a vector whose elements are the sensor measurements of different joints at a fixed time instance.

The Ballet data set contains 44 real video sequences of eight actions collected from an instructional ballet DVD [46]. Fig. 3 presents the sample frames of each action. We concatenate the randomly selected 10 sequences into a single long video sequence. The original resolution of each frame is 301×301. To speed up the computation, we first downsample each frame to the size of 80×30. Then, we build a dictionary of the frames with 300 bases using the Orthogonal matching Pursuit (OMP) algorithm [41] and encode each frame as a 300 dimensional sparse vector.

The Keck dataset consists of 14 different naval body gestures performed by three subjects. Fig. 4 shows the binary images of the some of the gestures of one subject in the dataset. The original resolution of each frame is 480×640. Following [23], to speed up the computation, we first downsample each binary image (frame) to the size of 80×106. Then, we compute the Euclidean distance transform [44] as frame-level features. After that, we build a dictionary of temporal words with 100 clusters using the k-means clustering, and encode each frame as a 100 dimensional binary vector. Finally, we concatenate the 14 gesture video sequences of each subject into a single long video sequence. For comparison purposes, we contrast our proposed method (**PM**) with three baseline subspace clustering methods **SSC** [7], **LRR** [24], and **LSR** [29], and two state-of-the-art temporal subspace clustering methods **OSC** [40] and **TSC**[3] [23].

In all the experiments, we use the clustering accuracy (ACC) and normalized mutual information (NMI) as the evaluation metrics.

4.1. Hyper-Parameter Setting

For the EM algorithm, we set the truncation level for the number of subspaces and their dimension to $(K = 20, S = 30)$ for the Mocap dataset, $(K = 15, S = 10)$ for the Ballet dataset, and $(K = 30, S = 50)$ for the Keck dataset. The hyper-parameters a, b of the Beta distributions are set with $a = K$ and $b = K/2$ (other settings of a and b yield similar results). The parameters for the EM algorithm are initialized

[2]Due to the lack of space, the video scene segmentation results are available in the Supplementary material.

[3]The MATLAB codes for **SSC** , **LRR**, **LSR**, **OSC**, and **TSC** are obtained from http://www.ccs.neu.edu/home/eelhami/codes.htm, https://sites.google.com/site/guangcanliu/, https://sites.google.com/site/canyilu/codes, https://github.com/sjtrny/OSC, and https://sites.google.com/site/lisheng1989/home/Publications, respectively

Table 2. ACC with standard deviation on Subjects of Mocap dataset. The best (bold red), the second best (red).

method	Subject-13	Subject-49	Subject-54	Subject-80	Subject-113
SSC	56.88 ± 2.01	85.47 ± 1.45	67.89 ± 2.33	59.04 ± 2.60	52.90 ± 2.27
LRR	57.18 ± 1.99	84.79 ± 1.78	68.81 ± 2.55	56.19 ± 2.50	53.35 ± 2.10
LSR	56.44 ± 2.16	82.27 ± 1.50	66.73 ± 1.90	**67.10** ± 2.13	52.55 ± 2.16
OSC	60.66 ± 1.88	88.25 ± 1.70	70.58 ± 1.67	63.14 ± 2.03	68.79 ± 2.08
TSC	67.92 ± 2.00	95.99 ± 1.33	76.38 ± 2.00	66.33 ± 2.33	76.28 ± 2.10
PM (our)	**74.75** ± 2.22	**98.79** ± 1.88	**81.43** ± 1.59	65.82 ± 2.49	**79.50** ± 2.18

Table 3. NMI with standard deviation on Subjects of Mocap dataset. The best (bold red), the second best (red).

method	Subject-13	Subject-49	Subject-54	Subject-80	Subject-113
SSC	0.5478 ± 0.023	0.7052 ± 0.016	0.6961 ± 0.028	0.5921 ± 0.029	0.6821 ± 0.035
LRR	0.5529 ± 0.030	0.6961 ± 0.020	0.6748 ± 0.020	0.6127 ± 0.032	0.6893 ± 0.029
LSR	0.5627 ± 0.027	0.7014 ± 0.013	0.6861 ± 0.018	0.6049 ± 0.030	0.6728 ± 0.033
OSC	0.6139 ± 0.019	0.8341 ± 0.017	0.7072 ± 0.022	0.6038 ± 0.025	0.7150 ± 0.025
TSC	0.6759 ± 0.020	0.9015 ± 0.015	0.7483 ± 0.024	0.6739 ± 0.019	0.7962 ± 0.029
PM (our)	**0.7532** ± 0.024	**0.9812** ± 0.019	**0.8453** ± 0.024	**0.7631** ± 0.023	**0.8767** ± 0.023

Table 4. Clustering accuracies (with standard derivation) on Ballet dataset. The best (bold red), the second best (red).

method	ACC	NMI
SSC	38.47 ± 3.07	0.3731 ± 0.023
LRR	35.15 ± 2.82	0.3923 ± 0.019
LSR	37.02 ± 3.21	0.4201 ± 0.020
OSC	41.04 ± 1.68	0.4008 ± 0.019
TSC	49.56 ± 2.31	0.5031 ± 0.013
PM (our)	**53.46** ± 2.99	**0.6206** ± 0.022

Table 5. Clustering accuracies (with standard derivation) on Keck dataset. The best (bold red), the second best (red).

method	ACC	NMI
SSC	27.32 ± 3.41	0.3058 ± 0.038
LRR	15.03 ± 3.26	0.1159 ± 0.069
LSR	37.17 ± 2.52	0.3429 ± 0.021
OSC	43.02 ± 2.57	0.4832 ± 0.025
TSC	**56.87** ± 2.92	0.6583 ± 0.020
PM (our)	55.49 ± 2.43	**0.6711** ± 0.027

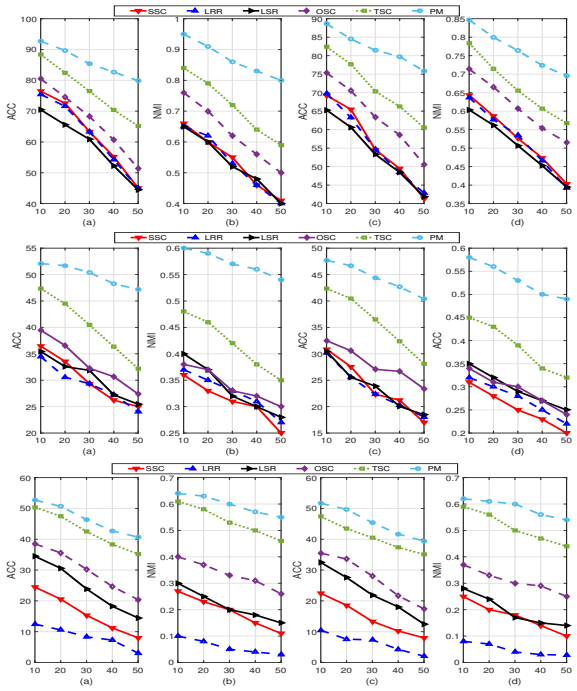

Figure 5. The results of different methods on datasets when the data suffer from the loss of features. First row: Subject 49 of the Mocap dataset. Second row: Ballet dataset. Third row: Keck dataset. Horizontal axes denote the missing rates (%). (a),(b): ACC and NMI results for MAR features, respectively. (c),(d): ACC and NMI results for NMAR features, respectively.

using a simple k-subspace algorithm [43]. For all the compared methods, we have tuned the parameters to get their best performance.

4.2. Results

The mean performance along with the standard deviation of each method over 5 runs on the different subjects of the three datasets is shown in Tables 2−5, from which we can infer two major points. (i) Clearly, the temporal subspace clustering methods (**PM**, **OSC**, **TSC**) outperform the standard subspace clustering methods (**SSC**, **LRR**, **LSR**) because they can exploit the temporal dependency in the data. (ii) our proposed method also outperforms the state of the art temporal **OSC** and **TSC** methods. We attribute this

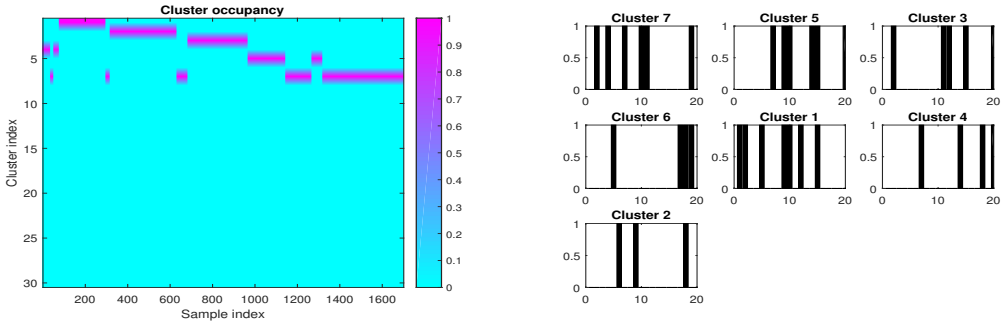

(a) Cluster index for each data point. (b) the subspace usage of each cluster (z_s)

Figure 6. Inferred model complexity for Subject 13 of Mocap dataset.

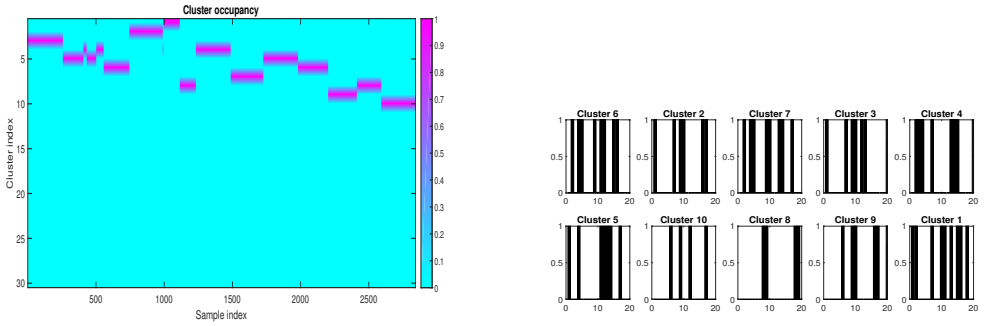

(a) Cluster index for each data point. (b) the subspace usage of each cluster (z_s)

Figure 7. Inferred model complexity for Subject 113 of Mocap dataset.

gain in performance to the probabilistic nature of the proposed method, making it more robust to outliers and noise in the datasets, in contrast to the optimization-based **OSC** and **TSC** methods.

4.3. Model Interpretation

Figs. 6 and 7 examine the number of inferred subspaces, as well as the number of bases for each subspace for the subjects 13 and 113 of the Mocap dataset. As can be seen the model infers 7 and 10 subspaces for the subjects 13 and 113, respectively. For each cluster (subspace) the subspace dimension is between 4 to 10 for the subject 13, and is between 5 to 15 for the subject 113.

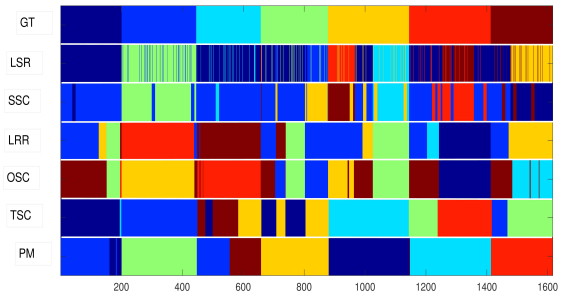

Figure 8. Clustering results on Subject 54 in Mocap dataset. Different colors denote different actions (GT stands for Ground Truth).

In Fig. 8 we contrast the clustering performance of competing methods on Subject 54 of Mocap dataset. As can be seen, **SSC**, **LRR** and **LSR** can not obtain meaningful temporal segments, as they do not consider the temporal information. On the other hand, **OSC**, **TSC** and our method could obtain more coherent temporal segments. Furthermore, because of the proposed **GP-GEM** prior for temporal data, our model can correctly recover the subspace structures in temporal space, hence, it reveals more clear sequential subspace structures than OSC and TSC.

4.4. Missing data Experiments

To demonstrate that our method can deal with the partially observed data gracefully, we conduct experiments by considering two contexts for missing data; the case when the values in data are missing at random (MAR) and the case when the values in data are missing not-at-random (MNAR).

Since the competing methods are not designed to deal

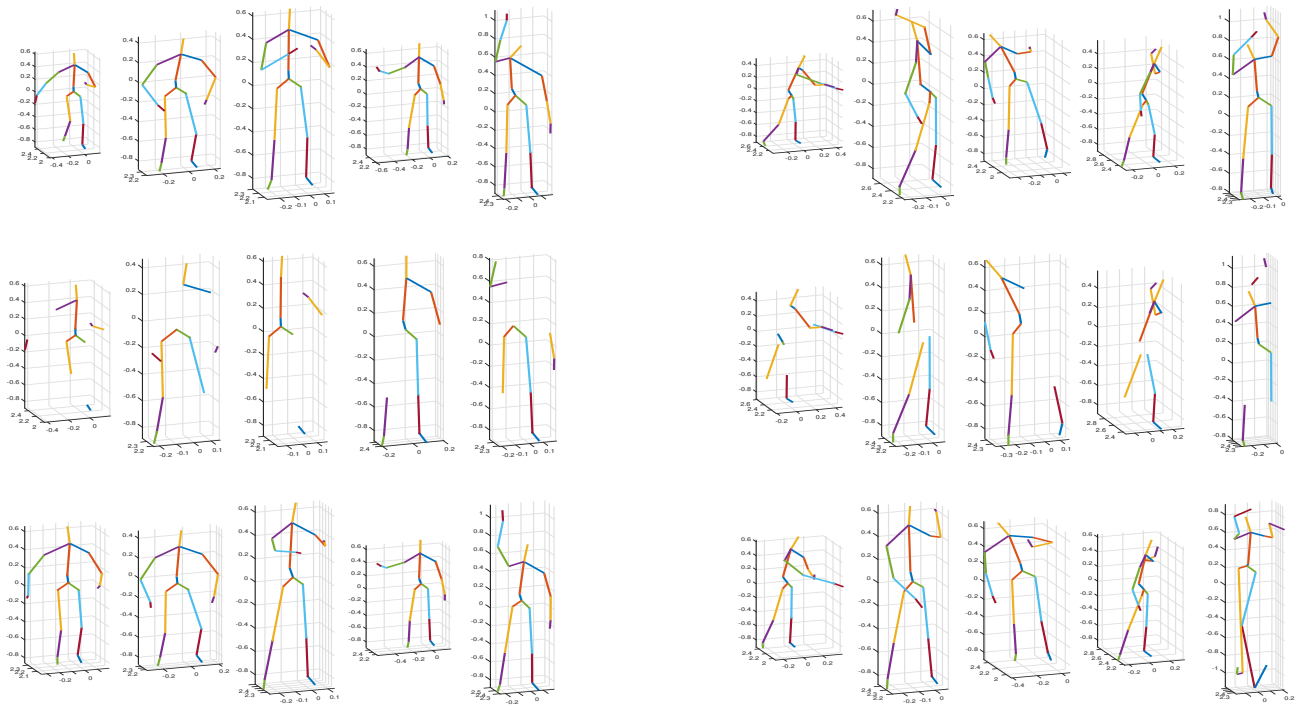

Figure 9. The reconstruction results for Subject 13 of Mocap dataset. From top to bottom: Original frames, original frames with 5 markers missing, recovered frames.

with missing data, we use zeros to replace the missing values, which has been shown [53] to have better performance than other filling-in techniques. For the MNAR setting, we conduct experiments by removing 20×20 squares form different locations in the data matrices repeatedly until the total fraction of the missing values is no less than the pre-specified missing rate. Fig. 5 shows the clustering results (average over 5 runs) of all methods under the MAR and MNAR setting on the Subject 49 of the Mocap dataset, Ballet dataset, and Keck dataset (missing data experiments for other subjects of Mocap dataset are available in the Supplementary material). As can be seen, although the error for the MNAR case tends to be larger than in the MAR case, our probabilistic method is much more robust, particularly for the large number of missing values) than all the competing methods under different amounts of missing values.

To further investigate the reconstruction ability of our probabilistic model for missing feature scenario, we use Subject 13 of the Mocap dataset.

For this experiment, we randomly remove 5 markers (each marker corresponds to a three dimensional spatial coordinates of a human body joint) representing different body segments from each frame. Then, we recover each frame using Eq. 3.1. Since the competing methods are not suitable for recovering the missing features, we do not compare them in this experiment. Fig. 9 show the recovery results of the **PM** on some of the frames. The first row shows 5 randomly selected frames taken from Subject 13 of the Mocap dataset. The second row shows the same frames with 5 markers missing. Finally, the last row of the figures gives recovered frames provided by the results of our model. As can be seen, the reconstructed missing values result in poses close to the actual body postures.

5. Conclusion

In this paper, we have proposed a novel probabilistic temporal subspace clustering model by incorporating the temporal information into the model's prior distribution that is capable of inferring the number of subspaces and their dimensions simultaneously from the available data. The temporal dependency is captured by establishing the cluster indices via a Gaussian process field followed by logistic functions. A specific kernel function is also employed to alleviate the computational issues raised by using the GPs. The experiments on three benchmark datasets demonstrate that our probabilistic method outperforms other state-of-the-art subspace clustering algorithms.

References

[1] M. Abavisani and V. M. Patel. Domain adaptive subspace clustering. 1

[2] S. D. Babacan, S. Nakajima, and M. Do. Probabilistic low-rank subspace clustering. In *Advances in Neural Information Processing Systems (NIPS)*, pages 2744–2752, 2012. 1

[3] J. Chen, H. Zhang, H. Mao, Y. Sang, and Z. Yi. Symmetric low-rank representation for subspace clustering. *Neurocomputing*, 173:1192–1202, 2016. 1

[4] Y. Cheng, Y. Wang, M. Sznaier, and O. Camps. Subspace clustering with priors via sparse quadratically constrained quadratic programming. In *IEEE Conference on Computer Vision and Pattern Recognition (CVPR)*, 2016. 1

[5] Z. Ding and Y. Fu. Robust multi-view subspace learning through dual low-rank decompositions. In *Thirtieth AAAI Conference on Artificial Intelligence (AAAI)*, 2016. 1

[6] E. Elhamifar and R. Vidal. Sparse subspace clustering. In *Conference on Computer Vision and Pattern Recognition (CVPR)*, pages 2790–2797. IEEE, 2009. 1

[7] E. Elhamifar and R. Vidal. Sparse subspace clustering: Algorithm, theory, and applications. *Pattern Analysis and Machine Intelligence, IEEE Transactions on*, 35(11):2765–2781, 2013. 1, 5

[8] Z. Fan, J. Zhou, and Y. Wu. Motion segmentation based on independent subspace analysis. In *Asian Conference on Computer Vision (ACCV)*, 2004. 1

[9] J. Feng, Z. Lin, H. Xu, and S. Yan. Robust subspace segmentation with block-diagonal prior. In *Proceedings of the IEEE Conference on Computer Vision and Pattern Recognition (CVPR)*, pages 3818–3825, 2014. 1

[10] Z. Ghahramani, G. E. Hinton, et al. The em algorithm for mixtures of factor analyzers. Technical report, CRG-TR-96-1, University of Toronto, 1996. 4

[11] X. Guo. Robust subspace segmentation by simultaneously learning data representations and their affinity matrix. In *International Joint Conference on Artificial Intelligence (IJCAI)*, pages 3547–3553, 2015. 1

[12] R. He, L. Wang, Z. Sun, Y. Zhang, and B. Li. Information theoretic subspace clustering. *IEEE Trans Neural Network Learning Systems*, 2015. 1

[13] R. He, Y. Zhang, Z. Sun, and Q. Yin. Robust subspace clustering with complex noise. *Image Processing, IEEE Transactions on*, 24(11):4001–4013, 2015. 1

[14] R. Heckel and H. Bölcskei. Robust subspace clustering via thresholding. *IEEE Transactions on Information Theory*, 61(11):6320–6342, 2015. 1

[15] M.-P. Hosseini, A. Hajisami, and D. Pompili. Real-time epileptic seizure detection from eeg signals via random subspace ensemble learning. In *Autonomic Computing (ICAC), 2016 IEEE International Conference on*, pages 209–218. IEEE, 2016. 1

[16] H. Hu, J. Feng, and J. Zhou. Exploiting unsupervised and supervised constraints for subspace clustering. *Pattern Analysis and Machine Intelligence, IEEE Transactions on*, 37(8):1542–1557, 2015. 1

[17] H. Ishwaran and L. F. James. Gibbs sampling methods for stick-breaking priors. *Journal of the American Statistical Association*, 2011. 2, 3

[18] P. Ji, M. Salzmann, and H. Li. Shape interaction matrix revisited and robustified: Efficient subspace clustering with corrupted and incomplete data. In *Proceedings of the IEEE International Conference on Computer Vision (ICCV)*, pages 4687–4695, 2015. 1

[19] M. I. Jordan, Z. Ghahramani, T. S. Jaakkola, and L. K. Saul. An introduction to variational methods for graphical models. *Machine learning*, 37(2):183–233, 1999. 4

[20] M. Lee, J. Lee, H. Lee, and N. Kwak. Membership representation for detecting block-diagonal structure in low-rank or sparse subspace clustering. In *Proceedings of the IEEE Conference on Computer Vision and Pattern Recognition (CVPR)*, pages 1648–1656, 2015. 1

[21] B. Li, Y. Zhang, Z. Lin, and H. Lu. Subspace clustering by mixture of gaussian regression. In *Proceedings of the IEEE Conference on Computer Vision and Pattern Recognition (CVPR)*, pages 2094–2102, 2015. 1

[22] C.-G. Li and R. Vidal. Structured sparse subspace clustering: A unified optimization framework. In *Proceedings of the IEEE Conference on Computer Vision and Pattern Recognition (CVPR)*, pages 277–286, 2015. 1

[23] S. Li, K. Li, and Y. Fu. Temporal subspace clustering for human motion segmentation. In *Proceedings of the IEEE International Conference on Computer Vision (ICCV)*, pages 4453–4461, 2015. 1, 2, 5

[24] G. Liu, Z. Lin, and Y. Yu. Robust subspace segmentation by low-rank representation. In *International Conference on Machine Learning (ICML)*, pages 663–670, 2010. 1, 5

[25] G. Liu, H. Xu, and S. Yan. Exact subspace segmentation and outlier detection by low-rank representation. In *International conference on artificial intelligence and statistics (AISTATS)*, pages 703–711, 2012. 1

[26] G. Liu and S. Yan. Latent low-rank representation for subspace segmentation and feature extraction. In *IEEE International Conference on Computer Vision (ICCV)*, pages 1615–1622. IEEE, 2011. 1

[27] C. Lu, J. Feng, Z. Lin, and S. Yan. Correlation adaptive subspace segmentation by trace lasso. In *Proceedings of the IEEE International Conference on Computer Vision (ICCV)*, pages 1345–1352, 2013. 1

[28] C. Lu, J. Tang, M. Lin, L. Lin, S. Yan, and Z. Lin. Correntropy induced l2 graph for robust subspace clustering. In *Proceedings of the IEEE International Conference on Computer Vision (ICCV)*, pages 1801–1808, 2013. 1

[29] C.-Y. Lu, H. Min, Z.-Q. Zhao, L. Zhu, D.-S. Huang, and S. Yan. Robust and efficient subspace segmentation via least squares regression. In *European Conference on Computer Vision (ECCV)*, pages 347–360. Springer, 2012. 1, 5

[30] Y. Ni, J. Sun, X. Yuan, S. Yan, and L.-F. Cheong. Robust low-rank subspace segmentation with semidefinite guarantees. In *IEEE International Conference on Data Mining Workshops (ICDMW),*, pages 1179–1188. IEEE, 2010. 1

[31] V. M. Patel, H. Van Nguyen, and R. Vidal. Latent space sparse and low-rank subspace clustering. *IEEE Journal of Selected Topics in Signal Processing*, 9(4):691–701, 2015. 1

[32] C. Peng, Z. Kang, H. Li, and Q. Cheng. Subspace clustering using log-determinant rank approximation. In *Proceedings of SIGKDD International Conference on Knowledge Discovery and Data Mining (KDD)*, pages 925–934. ACM, 2015. 1

[33] X. Peng, Z. Yi, and H. Tang. Robust subspace clustering via thresholding ridge regression. In *AAAI Conference on Artificial Intelligence (AAAI)*, pages 3827–3833, 2015. 1

[34] X. Peng, L. Zhang, and Z. Yi. Scalable sparse subspace clustering. In *Proceedings of the IEEE Conference on Computer Vision and Pattern Recognition (CVPR)*, pages 430–437, 2013. 1

[35] D.-S. Pham, S. Budhaditya, D. Phung, and S. Venkatesh. Improved subspace clustering via exploitation of spatial constraints. In *IEEE Conference on Computer Vision and Pattern Recognition (CVPR)*, pages 550–557. IEEE, 2012. 1

[36] G. Rybicki. Notes on gaussian random functions with exponential correlation functions (ornsteinuhlenbeck process). 1994. 3

[37] M. Soltanolkotabi, E. Elhamifar, E. J. Candes, et al. Robust subspace clustering. *The Annals of Statistics*, 42(2):669–699, 2014. 1

[38] A. Taalimi, A. Rahimpour, C. Capdevila, Z. Zhang, and H. Qi. Robust coupling in space of sparse codes for multi-view recognition. In *Image Processing (ICIP), 2016 IEEE International Conference on*, pages 3897–3901. IEEE, 2016. 1

[39] R. Thibaux and M. I. Jordan. Hierarchical beta processes and the indian buffet process. In *International conference on artificial intelligence and statistics (AISTATS)*, pages 564–571, 2007. 2, 3

[40] S. Tierney, J. Gao, and Y. Guo. Subspace clustering for sequential data. In *Proceedings of the IEEE Conference on Computer Vision and Pattern Recognition (CVPR)*, pages 1019–1026, 2014. 2, 5

[41] J. A. Tropp and A. C. Gilbert. Signal recovery from random measurements via orthogonal matching pursuit. *IEEE Transactions on information theory*, 53(12):4655–4666, 2007. 5

[42] R. Vidal, Y. Ma, and S. Sastry. Generalized principal component analysis (gpca). *Pattern Analysis and Machine Intelligence, IEEE Transactions on*, 27(12):1945–1959, 2005. 1

[43] D. Wang, C. Ding, and T. Li. K-subspace clustering. In *Machine learning and knowledge discovery in databases*, pages 506–521. Springer, 2009. 6

[44] J. Wang and Y. Tan. Efficient euclidean distance transform algorithm of binary images in arbitrary dimensions. *Pattern recognition*, 46(1):230–242, 2013. 5

[45] S. Wang, X. Yuan, T. Yao, S. Yan, and J. Shen. Efficient subspace segmentation via quadratic programming. In *AAAI Conference on Artificial Intelligence (AAAI)*, volume 1, pages 519–524, 2011. 1

[46] Y. Wang and G. Mori. Human action recognition by semilatent topic models. *IEEE transactions on pattern analysis and machine intelligence*, 31(10):1762–1774, 2009. 5

[47] Y. Wang, Y.-X. Wang, and A. Singh. Clustering consistent sparse subspace clustering. *arXiv preprint arXiv:1504.01046*, 2015. 1

[48] Y. Wang, Y.-X. Wang, and A. Singh. Graph connectivity in noisy sparse subspace clustering. In *Proceedings of the 19th International Conference on Artificial Intelligence and Statistics (AISTATS)*, pages 538–546, 2016. 1

[49] Y. Wang and J. Zhu. Dp-space: Bayesian nonparametric subspace clustering with small-variance asymptotics. In *International Conference on Machine Learning (ICML)*, pages 862–870, 2015. 1

[50] X. Wen, L. Qiao, S. Ma, W. Liu, and H. Cheng. Sparse subspace clustering for incomplete images. In *IEEE International Conference on Computer Vision Workshops (CVPRW)*, pages 19–27, 2015. 1

[51] C. K. Williams and C. E. Rasmussen. Gaussian processes for machine learning. *the MIT Press*, 2(3):4, 2006. 2, 3

[52] F. Wu, Y. Hu, J. Gao, Y. Sun, and B. Yin. Ordered subspace clustering with block-diagonal priors. *IEEE Transaction on Cybernetics*, 19(1):475–492, 2015. 2

[53] C. Yang, D. Robinson, and R. Vidal. Sparse subspace clustering with missing entries. In *International Conference on Machine Learning (ICML)*, pages 2463–2472, 2015. 1, 8

[54] Y. Yang, J. Feng, N. Jojic, J. Yang, and T. S. Huang. l_0-sparse subspace clustering. In *European Conference on Computer Vision (ECCV)*, pages 731–747. Springer, 2016. 1

[55] M. Yin, J. Gao, Z. Lin, Q. Shi, and Y. Guo. Dual graph regularized latent low-rank representation for subspace clustering. *Image Processing, IEEE Transactions on*, 24(12):4918–4933, 2015. 1

[56] M. Yin, Y. Guo, J. Gao, Z. He, and S. Xie. Kernel sparse subspace clustering on symmetric positive definite manifolds. *IEEE Conference on Computer Vision and Pattern Recognition (CVPR)*, 2016. 1

[57] M. Yin, Y. Guo, J. Gao, Z. He, and S. Xie. Kernel sparse subspace clustering on symmetric positive definite manifolds. In *The IEEE Conference on Computer Vision and Pattern Recognition (CVPR)*, June 2016. 1

[58] C. You, C.-G. Li, D. P. Robinson, and R. Vidal. Oracle based active set algorithm for scalable elastic net subspace clustering. *IEEE Conference on Computer Vision and Pattern Recognition (CVPR)*, 2016. 1

[59] C. You, D. Robinson, and R. Vidal. Scalable sparse subspace clustering by orthogonal matching pursuit. In *IEEE Conference on Computer Vision and Pattern Recognition*, volume 1, 2016. 1

[60] X.-T. Yuan and P. Li. Sparse additive subspace clustering. *European Conference on Computer Vision (ECCV)*, pages 644–659, 2014. 1

[61] X. Zhang, D. Phung, S. Venkatesh, D.-S. Pham, and W. Liu. Multi-view subspace clustering for face images. In *Digital Image Computing: Techniques and Applications (DICTA), 2015 International Conference on*, pages 1–7. IEEE, 2015. 1

[62] V. Zografos, L. Ellis, and R. Mester. Discriminative subspace clustering. In *Proceedings of the IEEE Conference on Computer Vision and Pattern Recognition (CVPR)*, pages 2107–2114, 2013. 1